[Atmospheric Chemistry and Physics]

Supporting Information for

Injection Near the Stratopause Minimizes the Stratospheric Side Effects of Sulfur-Based Climate Intervention

Pengfei Yu[1]*, Yifeng Peng[2], Karen H. Rosenlof[3], Ru-Shan Gao[3,4], Robert W. Portmann[3], Martin Ross[5], Eric Ray[3,4], Jianchun Bian[6], Simone Tilmes[7] and Owen B. Toon[8]

[1] Institute for Environmental and Climate Research, College of Environment and Climate, Jinan University, Guangzhou, China

[2] School of Atmospheric Sciences, Lanzhou University, Lanzhou, China

[3] Chemical Science Laboratory, National Oceanic and Atmospheric Administration, Boulder, Colorado

[4] Cooperative Institute for Research in Environmental Sciences, University of Colorado Boulder, Boulder, CO, USA

[5] Civil and Commercial Launch Projects, The Aerospace Corporation, Los Angeles, California

[6] Key Laboratory of Middle Atmosphere and Global Environment Observation, Institute of Atmospheric Physics, Chinese Academy of Sciences, Beijing, China

[7] Atmospheric Chemistry, Observations, and Modeling Laboratory, National Center for Atmospheric Research, Boulder, Colorado

[8] Department of Atmospheric and Oceanic Sciences and Laboratory for Atmospheric and Space Physics, University of Colorado, Boulder, Colorado

Correspondence to: Pengfei Yu (pengfei.yu@colorado.edu)

Contents of this file
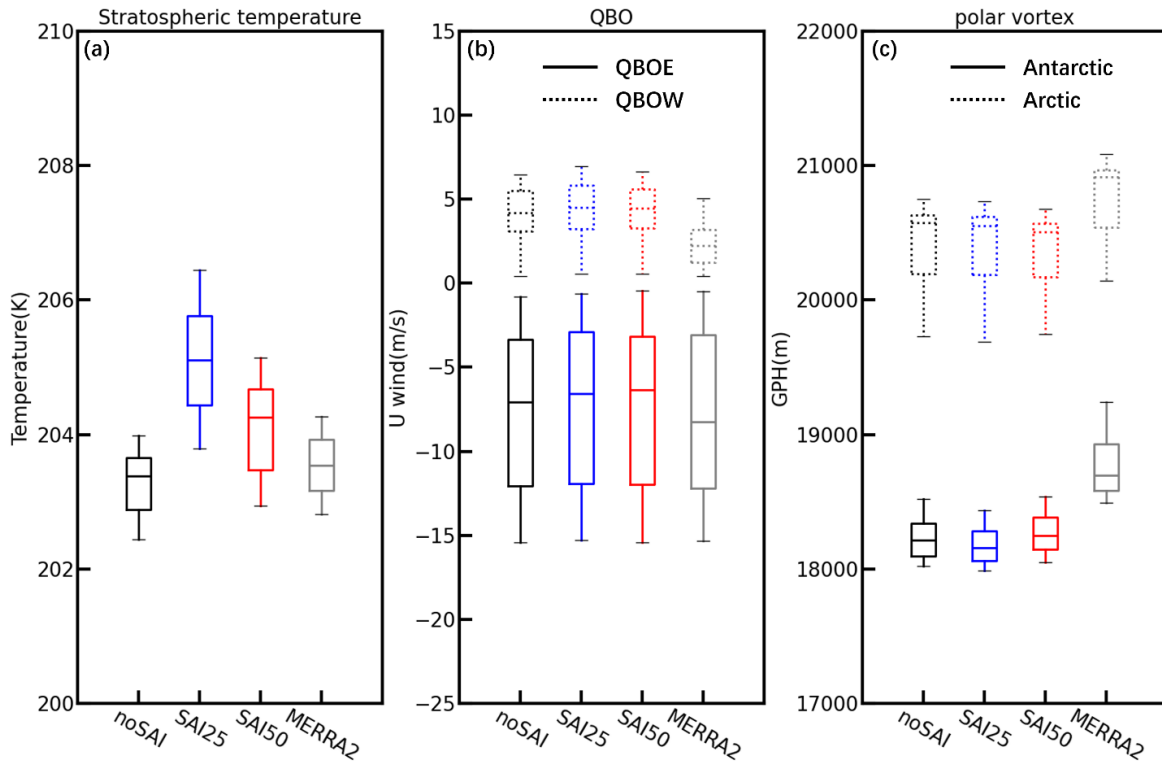
Figure S1: Box plots comparing stratospheric variability between model simulations and MERRA2 reanalysis (2000-2020). (a) near-global (60°S-60°N) temperatures at 100 mb; (b) QBO strength (tropical zonal mean zonal wind at 50 mb); (c) Antarctic polar vortex strength (denoted by the geopotential height averaged over 65°S-90°S at 50 mb) in the model and MERRA2 reanalysis dataset between year 2000 and 2020. Box plots show the median (horizontal line), 25th-75th percentiles (box), and 5th-95th percentiles (whiskers).
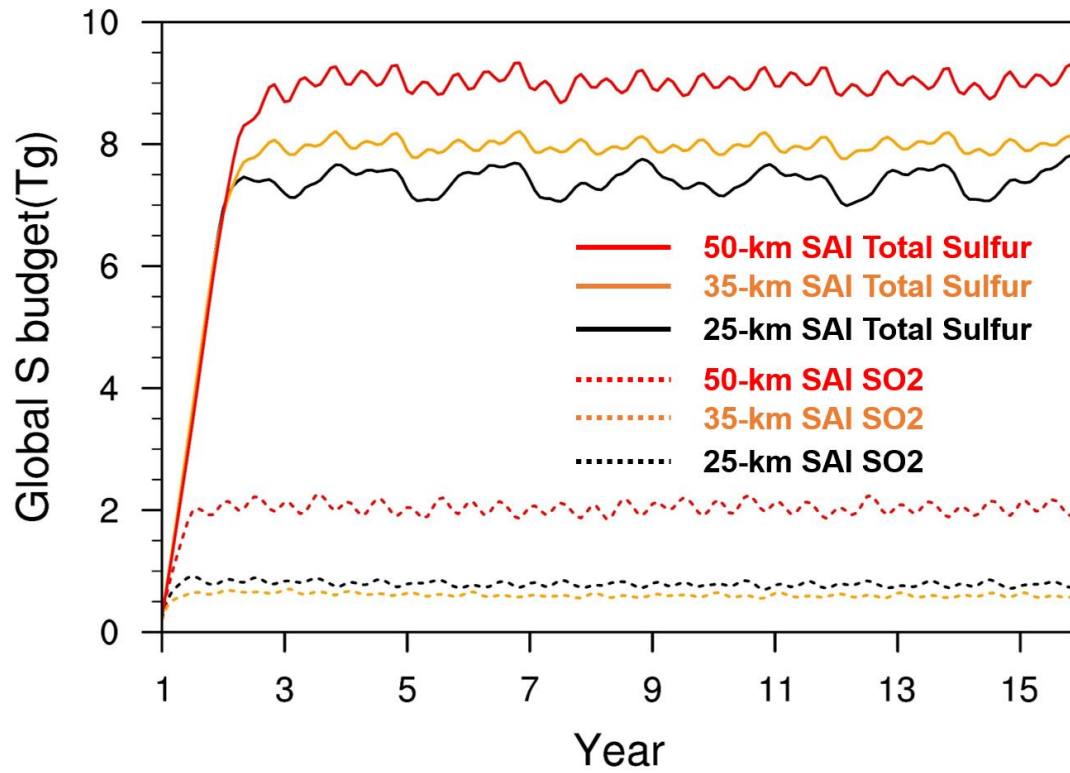
Figure S2: Simulated global stratospheric budget of sulfur (Tg) in SAI experiments with injection heights of 25, 35 and 50 km at 15°N and 15°S. The budget of total sulfur (both in gas and condensed phases) is denoted by solid lines, and the budget of SO_2 gas is denoted by the dashed lines.
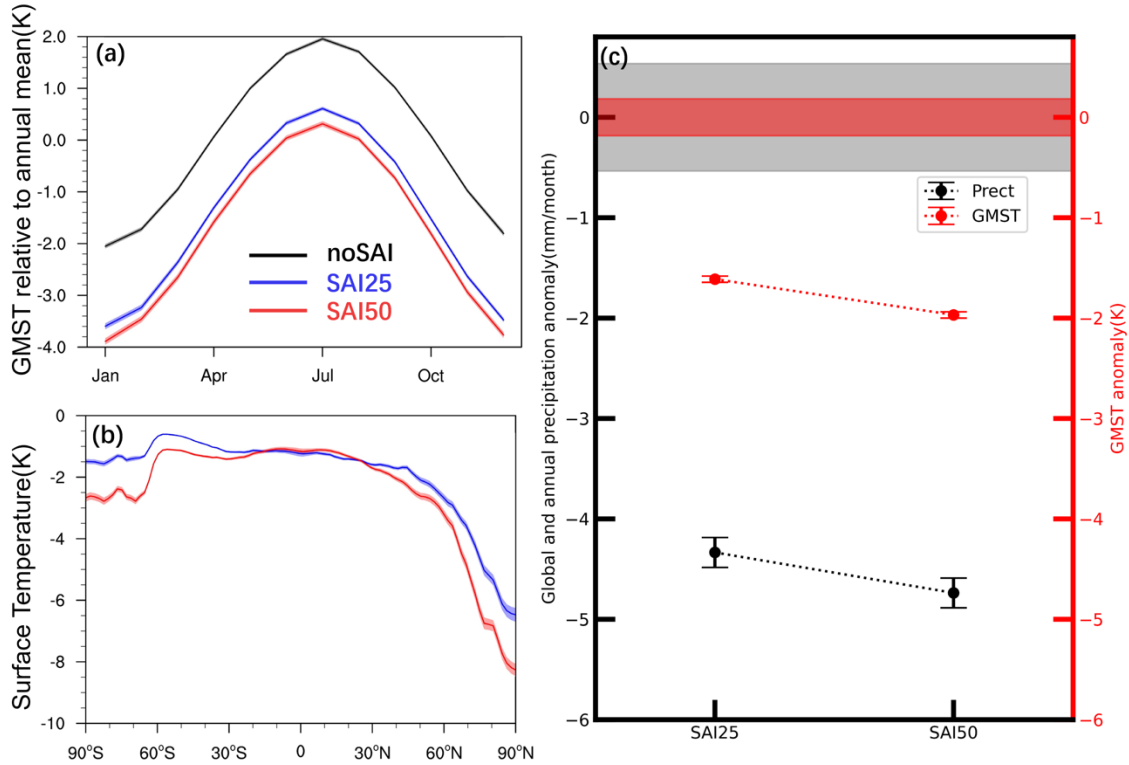
Figure S3: Global surface temperature responses to SAI scenarios. (a) Seasonal cycle of global mean surface temperature (GMST) relative to the annual mean among control (in black), SAI_{25} (in blue) and SAI_{50} (in red) simulations. The shadings of each line represent the ensemble standard deviation of the mean; (b) zonal mean surface temperature anomalies relative to the control simulations for SAI_{50} (red) and SAI_{25} (blue) scenarios. The shadings of each line represent the ensemble standard deviation of the mean; (c) GMST anomalies for SAI_{25} and SAI_{50} scenarios (red dots, right axis) with error bars showing ensemble standard deviation of the mean from 45-member simulations. Global mean precipitation anomaly for SAI_{25} and SAI_{50} scenario (black dots, left axis) with error bars showing ensemble standard deviation of the mean. The magnitude of natural variabilities (one standard deviation) of GMST and precipitation rate from the control simulations are shown in red and black shadings, respectively.
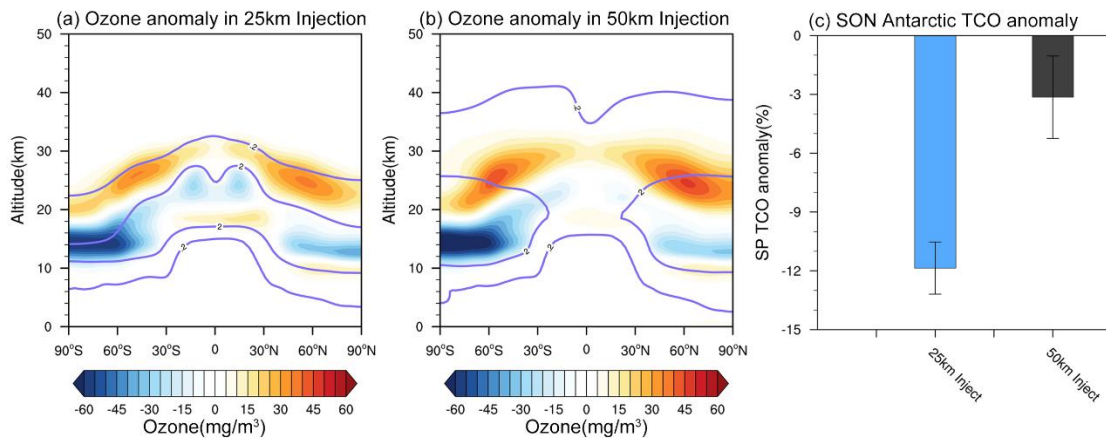
Figure S4: (a) Simulated annual mean ozone anomalies due to 25-km injection SAI under the ozone depleting substance (ODS) conditions of year 2040 relative to the simulations without SAI. The simulated annual mean aerosol concentrations of 12 and 2 mg m^{-3} are denoted by the contour lines; (b) same as (a) but for the simulated ozone anomalies due to 50-km injection SAI (SAI$_{50}$); (c) Simulated Antarctic (60°S-90°S) column ozone anomaly averaged from September-October-November (SON) from SAI scenarios with different injection altitudes (at 25 km and 50 km) under the ODS conditions of year 2040. The error bars denote the standard deviation of the mean from the ensemble simulations with details in Materials and Methods.